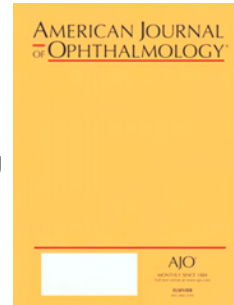


# Journal Pre-proof

Sector Retinitis Pigmentosa: Extending the Molecular Genetics Basis and Elucidating the Natural History

Michalis Georgiou, Parampal S. Grewal, Akshay Narayan, Muath Alser, Naser Ali, Kaoru Fujinami, Andrew R. Webster, Michel Michaelides



PII: S0002-9394(20)30423-2

DOI: <https://doi.org/10.1016/j.ajo.2020.08.004>

Reference: AJOPHT 11504

To appear in: *American Journal of Ophthalmology*

Received Date: 27 May 2020

Revised Date: 29 July 2020

Accepted Date: 3 August 2020

Please cite this article as: Georgiou M, Grewal PS, Narayan A, Alser M, Ali N, Fujinami K, Webster AR, Michaelides M, Sector Retinitis Pigmentosa: Extending the Molecular Genetics Basis and Elucidating the Natural History, *American Journal of Ophthalmology* (2020), doi: <https://doi.org/10.1016/j.ajo.2020.08.004>.

This is a PDF file of an article that has undergone enhancements after acceptance, such as the addition of a cover page and metadata, and formatting for readability, but it is not yet the definitive version of record. This version will undergo additional copyediting, typesetting and review before it is published in its final form, but we are providing this version to give early visibility of the article. Please note that, during the production process, errors may be discovered which could affect the content, and all legal disclaimers that apply to the journal pertain.

© 2020 The Author(s). Published by Elsevier Inc.

## ABSTRACT

**Purpose:** To determine the genetic background of sector retinitis pigmentosa (RP), natural history, in order to better inform patient counselling.

**Design:** Retrospective case series.

**Methods:** Review of clinical notes, retinal imaging including color fundus photography (CFP), fundus autofluorescence (FAF), and optical coherence tomography (OCT), electrophysiological assessment (ERG), and molecular genetic testing was performed in patients with sector RP from a single tertiary referral center.

**Main Outcome Measures:** Reporting demographic data, signs and symptoms, visual acuity, molecular genetics, ERG, FAF and OCT findings.

**Results:** Twenty-six molecularly confirmed patients from 23 different families were identified, harboring likely disease-causing variants in nine genes. The mode of inheritance was autosomal recessive (AR, n=6: *USH1C*, n=2; *MYO7A*, n=2; *CDH3*, n=1; *EYS*, n=1), X-linked (XL, n=4: *PRPS1*, n=1; *RPGR*, n=3), and autosomal dominant (AD, n=16: *IMPDH1*, n=3; *RP1*, n=3; *RHO*, n=10), with a mean age of disease onset of 38.5, 30.5 and 39.0 years respectively. Five of these genes have not previously been reported to cause sector RP (*PRPS1*, *MYO7A*, *EYS*, *IMPDH1*, and *RP1*). Inferior and nasal predilection was common across the different genotypes and patients tended to maintain good central vision. Progression on serial FAF was observed in *RPGR*, *MYO7A*, *CDH23*, *EYS*, *IMPDH1*, *RP1* and *RHO*-associated sector RP.

**Conclusions:** The genotypic spectrum of the disease is broader than previously reported. The provided longitudinal data will help to provide more accurate patient prognosis and counselling, as well as inform patients' potential participation in the increasing numbers of trials of novel therapeutics and access to future treatments.

**Sector Retinitis Pigmentosa: Extending the Molecular Genetics Basis and Elucidating the Natural History**

Michalis Georgiou<sup>1,2</sup>, Parampal S. Grewal<sup>2</sup>, Akshay Narayan<sup>1</sup>, Muath Alser<sup>1</sup>, Naser Ali<sup>2</sup>, Kaoru Fujinami<sup>1,2,3</sup>, Andrew R. Webster<sup>1,2</sup>, Michel Michaelides<sup>1,2</sup>

<sup>1</sup> UCL Institute of Ophthalmology, University College London, London, UK

<sup>2</sup> Moorfields Eye Hospital, London, UK

<sup>3</sup> Laboratory of Visual Physiology, Division of Vision Research, National Institute of Sensory Organs, National Hospital Organization Tokyo Medical Center, Tokyo, Japan; Department of Ophthalmology, Keio University School of Medicine, Tokyo, Japan.

**Corresponding author:**

Michel Michaelides,  
UCL Institute of Ophthalmology,  
11-43 Bath Street, London, EC1V 9EL, UK.  
E-mail: michel.michaelides@ucl.ac.uk  
Tel. no: 004420 7608 6864

**Number of Figures:** 6

**Supplementary Materials:** 3 (2 tables, 1 figure)

**Running (Short) Title:** Sector Retinitis Pigmentosa

Supplemental Material available at AJO.com.

**Keywords:** fundus autofluorescence, FAF, optical coherence tomography, OCT, retina, retinitis pigmentosa, sector, sectorial, sectoral, RP, inherited retinal disease, dystrophy, genetics

Journal Pre-proof

## INTRODUCTION

Retinitis pigmentosa (RP) is a heterogeneous group of inherited retinal disorders (IRD), characterized by nyctalopia, visual field (VF) defects, and progressive retinal degeneration.<sup>1</sup> RP can also exist in syndromic forms, such as Usher syndrome and Bardet-Biedl syndrome.<sup>2</sup> Sector RP and pericentral RP are atypical variants of RP.<sup>3, 4</sup>

Sector RP was first reported in 1937, with limited subsequent reports in the literature, despite representing a distinct phenotype. It is characterized by typical clinical features of RP limited to one or two fundus quadrants.<sup>5</sup> It tends to affect inferior and nasal quadrants with corresponding superior VF defects.<sup>6</sup> Sector RP has a favourable visual prognosis compared to generalized RP, having been reported that 82% retain a visual acuity (VA) of 20/40 or better.<sup>7</sup> Autosomal dominant (AD), autosomal recessive (AR) and X-linked (XL) modes of inheritance have been reported. There are six previously reported disease-causing genes: rhodopsin (AD, *RHO*, OMIM 180380, n=70 cases),<sup>4, 6, 8-17</sup> usherin (AR, *USH1C*, OMIM 605242, n=2),<sup>2</sup> cadherin 23 (AR, *CDH23*, OMIM 605516, n=1),<sup>18</sup> retinol dehydrogenase 5 (AR, *RDH5*, OMIM 601617, n=1),<sup>19</sup> arrestin (AR, *SAG*, OMIM 181031, n=1),<sup>20</sup> and more recently RP GTPase regulator gene (X-linked, *RPGR*, OMIM 312610, n=2).<sup>4, 21</sup> All the previously reported sector RP causing variants are summarized in **Supplementary Table 1**. Currently there are ongoing efforts for the development and approval of novel therapeutic options for *RPGR*-RP and *RHO*-RP.<sup>22, 23</sup>

There are limited publications on sector RP, in particular longitudinal natural history studies are limited to case reports. Herein, we report the largest series and first longitudinal study in molecularly confirmed patients with sector RP. While sector RP is believed to be a mild condition compared to generalized RP, there is need for more robust data to advise on prognosis. This is particularly true in the molecular era and with the development of novel therapeutics.

The purpose of this study is therefore to investigate genetic and phenotypic variability in a large cohort of molecularly confirmed patients with sector RP seen in a tertiary center, as well as to investigate disease natural history and provide valuable information that can better inform patient counselling and prognostication.

## METHODS

### Patient Identification

All correspondence on the electronic clinical database (OpenEyes) at Moorfields Eye Hospital (MEH), London, UK was searched for the key words: “sector”, “sectorial”, and “sectoral”. The clinical notes of all the identified patients were reviewed to confirm the diagnosis of sector RP. All patients with a confirmed clinical diagnosis were seen in retinal genetics clinics and evaluated by experienced specialists (ARW and MM). The patients were identified in the MEH Inherited Eye Disease database for molecular confirmation. Patients were included in this database after obtaining informed consent. This study adhered to the tenets of the Declaration of Helsinki and was approved by the MEH ethics committee.

### Assessments

Medical notes and clinical images were reviewed, including dilated funduscopy, VA recording, electrophysiological assessment (ERG), retinal imaging including color fundus photography (CFP; Optos, California and TopCon), optical coherence tomography (OCT, Heidelberg Spectralis) and fundus autofluorescence (FAF, Heidelberg Spectralis and Optos California). The age of disease onset was defined as the age of the first disease related symptom(s). Full-field and pattern electroretinography were performed using gold foil electrodes to incorporate the International Society for Clinical Electrophysiology of Vision standards (ISCEV) in nine patients.

### Retinal Imaging

The retina was divided into four halves, with the center at the fovea: the superior-inferior and nasal-temporal meridians, defined the nasal and temporal retina, and the superior and inferior retina respectively (**Supplementary Figure 1**). FAF imaging (55 degrees) and CFP were used to evaluate the extent of retinal involvement. The presence of a perimacular ring of increased signal on FAF was also noted. Macular involvement was also investigated, using all available modalities. Interocular symmetry was evaluated qualitatively, taking into account the topology of the affected quadrants and the extent of degeneration. Eyes with different affected quadrants were defined as asymmetric.

Foveal total retinal thickness (FTRT) and outer nuclear layer (ONL) thickness were calculated at baseline and last follow-up. All measurements were made by a single examiner using the digital calipers built into the software (Heidelberg Eye Explorer; Heidelberg Engineering), and a 1-pixel:1- $\mu\text{m}$  display with maximum magnification. FTRT was measured as the distance between the internal limiting membrane (ILM) and the retinal pigment epithelium (RPE). ONL thickness was measured as the distance between the ILM and the external limiting membrane (ELM), or the distance between the outer plexiform layer (OPL) and the ELM, for patients without and with foveal hypoplasia respectively.

### Statistical Methods

The statistical analysis was carried out using SPSS Statistics (Chicago, IL, USA). Significance for all statistical tests was set at  $P < 0.05$ . The Shapiro-Wilk test was used to test for normality for all variables.

Journal Pre-proof

## RESULTS

### Patient Characteristics

Twenty-six molecularly confirmed patients were identified, from 23 pedigrees (as noted with Pedigree number on Table 1), harboring likely disease-causing variants in nine genes. The modes of inheritance were X-linked (XL, n=4: *PRPS1*, n=1; *RPGR*, n=3), autosomal recessive (AR, n=6: *USH1C*, n=2; *MYO7A*, n=2; *CDH23*, n=1; *EYS*, n=1), and autosomal dominant (AD, n=16: *IMPDH1*, n=3; *RP1*, n=3; *RHO*, n=10). Five of these genes have not previously been reported to cause sector RP (*PRPS1*, *MYO7A*, *EYS*, *IMPDH1*, and *RP1*). The molecular genetics, sex, and family history, of all patients are presented in **Table 1**. The clinical presentation including the age of disease onset, of each genotype are presented individually below. The two siblings with *USH1C* variants and sector RP were previously described in detail by Saihan et al,<sup>2</sup> and were excluded from OCT, FAF, and further individual analysis.

### Visual Acuity and Disease Symmetry

VA was available for 24 of the 26 patients. From the 24 patients, two had reduced VA in one eye, unrelated to retinal degeneration (P1: left eye - closed angle glaucoma and cataract, P19: right eye - amblyopia), and were excluded from VA interocular comparison. The mean VA at baseline examination (mean age: 42.8, range: 18.3-76.1) for the right and left eyes was 0.035 and 0.061 LogMAR respectively. VA was similar between right and left eyes ( $P=0.203$ ,  $t=-1.31$ ,  $df=21$ ). Twenty patients had longitudinal VA assessment, with a mean follow-up of 10.6 years (range: 2.3-36.1 years). Final mean VA was 0.06 and 0.10 LogMAR for right and left eyes respectively. VA was statistically significantly worse at follow-up ( $P=0.007$ ,  $t=-3.05$ ,  $df=19$ ). **Figure 1** presents the VA for all patients over time, with genotype details.

In all patients evaluated for interocular symmetry (n=25), the disease was symmetric between eyes in 23 patients (92%), in terms of the available CFP, OCT and FAF. **Figure 2** presents FAF examples of interocular symmetry for all genotypes, with the exception of *PRPS1*. While *PRPS1* is known to cause asymmetric disease in females,<sup>24</sup> imaging data was only available from the right eye (due to dense left cataract and prior left angle closure) precluding interocular comparison (**Figure 3A**). The two other patients (P3-*RPGR* and P17-*RHO*) with intraocular difference in presentation were only noted on wide-field imaging (**Figure 3B-C**).

### OCT Quantitative and Qualitative assessment

OCT imaging was performed at least once in 18 patients (mean age: 46 years, range: 18-90 years). Mean foveal thickness was 156  $\mu\text{m}$  and 152  $\mu\text{m}$  for right and left eyes respectively. Mean ONL thickness was 124  $\mu\text{m}$  and 120  $\mu\text{m}$  for right and left eyes respectively. Previously reported mean  $\pm$  SD from unaffected controls for ONL thickness are 112.9  $\pm$  15.2 (right eye) and 112.1  $\pm$  13.9  $\mu\text{m}$  (left eye).<sup>25</sup> One patient (5.6%, P4) had macular involvement, with loss of the macular ellipsoid zone (**Figure 4B**).

Thirteen patients had serial OCT assessment with a mean final follow-up of 5.6 years (range: 4.4-8.1 years). Mean foveal thickness was 154  $\mu\text{m}$  and 152  $\mu\text{m}$  for right and left eyes respectively. Mean ONL thickness was 117  $\mu\text{m}$  and 112  $\mu\text{m}$  for right and left eyes respectively. Examples of OCT interocular symmetry and disease progression

are presented in **Figure 4**. Cystoid macular edema (CME) was observed in four patients (P2-*RPGR* (**Figure 4A**), P11-*IMPDH1*, P13-*IMPDH1* (**Figure 4D**) and P26-*RHO* (**Figure 4F**)), with one having XL (P2) and three AD (P11, P13, P26) inheritance mode. Three patients had epiretinal membrane (P2 (**Figure 4A**), P12 and P14). One patient had focal vitreomacular traction (VMT; P13, Stage 1 (**Figure 4D**)).

### Disease Localization and Evidence of Progression

FAF imaging was used for localization of the disease and investigation of structural progression, due to the peripheral nature of the disease and the wider field of view compared to OCT. Eighteen patients had 55 degree FAF imaging (mean age: 46 years old, range: 18.3-70.4 years old). Fifteen patients (83.3%) had peripapillary atrophic changes (**Figure 5 A-D and F-J**). The three patients without peripapillary changes were P7, P9 (**Figure 5E**) and P16, with *MYO7A*, *CDH23* and *RP1* genotypes respectively. A common finding was a hyperautofluorescent rim, bordering areas of affected and healthy retina (n=13, 72.2%, **Figures 2 and 5**). A peri-foveal ring of increased signal was present in two subjects (11.1%, P14-*RP1* (**Figure 5H**) and P26-*RHO* (**Figure 5J**)). Both of these patients had hyperautofluorescent rings and rims. Foveal involvement was observed only in one subject (P4-*RPGR*, **Figure 5C**). Disease localization was noted: i) nasal (n=1, 5.6%, P2-*RPGR* carrier, **Figure 5A**), ii) inferior (n=6, 33.3%), iii) inferior and nasal (n=9, 50%), and iv) inferior, temporal and nasal (n=2, 11.2%, P13-*IMPDH1* and P14-*RP1*). Disease localization for each individual patient is presented in **Supplementary Table 2**.

Sixteen patients had available follow-up imaging (mean follow-up time 5 years, range: 1-9.1 years). Seven of the 16 patients (43.8%), showed changes in the FAF signal. **Figure 5** presents all six patients with evidence of progression; the changes were peripheral and small in area, and most likely of limited clinical significance. Only one patient showed extension of the disease to the superior retina (P14-*RP1*), having a more “typical” RP presentation, with mid-peripheral changes in all quadrants (**Figure 5H**). The mean follow-up of the patients with structural changes was 5.6 years (range 4-7.8 years).

### X-linked Sector RP

#### *PRPS1* (n=1)

The patient (P1) was diagnosed at age 45 and presented with reduced vision. Vision in the left eye was perception of light and without clear visual axis, due to previous angle closure glaucoma. Inferior atrophy with pigmentary changes were documented on funduscopy. The VA in the right eye was 0.27 LogMAR at 76 years of age, and only mildly deteriorated to 0.48 LogMAR at 91 years of age. While no FAF imaging was available for disease localization; CFP documented the disease in the inferior retina (**Figure 3A**).

#### *RPGR* (n=3)

Three patients harbored *RPGR* variants in ORF15. One female carrier (P2) had an age of disease onset at 32 years, presenting with increased difficulty with night vision. VA was 0.24 and 0.18 LogMAR at 35 years of age and remained relatively stable at 0.18 and 0.3 LogMAR after 16 years of follow-up, for right and left eye respectively. The two

affected males had an earlier age of onset, at age 4 years (P3) and 10 years (P4), with the later diagnosed at asymptomatic screening by an optometrist and the former having reduced color vision. VA for P3 at 18 years of age was 0.18 LogMAR in both eyes. P4 at 37 years of age had a baseline VA of 0.18 LogMAR in both eyes, and over 13.5 years of follow-up deteriorated to 0.92 and 0.52 LogMAR in the right and left eye respectively. Greater disease progression and VA deterioration was observed in the right eye due to foveal involvement (**Figure 5C**). All three patients showed involvement of the inferior and nasal retina on FAF (**Figure 5A-C**). The affected female also had a tapetal-like reflex, a common finding among *RPGR*-carriers,<sup>26</sup> visible both on funduscopy and FAF (**Figure 2A**). P2 had ERG testing at age 34 years, showing generalized retinal dysfunction, affecting both the cone and the rod system, with macular involvement. Rod specific ERG was precluded by blink artefact. P3 had ERG testing at age 29 years, showing generalized retinal dysfunction, affecting more the rod than the cone system, with paracentral macular involvement. Interestingly the affected male cousin of P3, has a symmetrical, non-sectorial phenotype of cone-rod dystrophy, despite harboring the same *RPGR* variant.

#### **Autosomal Recessive Sector RP *MYO7A* (n=2)**

Patients P7 and P8, from two independent pedigrees and both severely hearing impaired, were referred for evaluation of pigmentary changes in the inferior retina after routine optometry assessment (**Figure 6A-B**), without any associated visual complaint, at age 53 and 45 years old respectively. Superior field defects were noted in both patients. VA for P7, was 0 and -0.08 LogMAR at age 57, and 0.0 and 0.16 LogMAR at age 62 years, for right and left eye respectively. VA for P8 was 0.0 LogMAR for both eyes at age 46, and 0.12 and 0.0 LogMAR for right and left eye after 15 years of follow-up. P7 had normal pattern and full-field ERGs at age 58 years, and P8 had normal pattern ERG, and mildly subnormal full-field ERG, with normal peak times, at 44 years of age.

#### ***CDH23* (n=1)**

P9 had Usher syndrome Type 1 and he was referred at 18 years of age for evaluation (**Figure 6C**). He had bilateral cochlear implants. VA was 0.0 and -0.08 LogMAR at 18 years of age, and 0.04 and 0.06 after six years of follow-up for the right and left eye respectively. Previous ERG testing at 7 years of age showed normal responses from both eyes, which deteriorated after 8 years of follow-up both for the rod and to a lesser extent the cone system.

#### ***EYS* (n=1)**

P10 when 54 years old was noted by her optometrist to have bilateral supero-temporal VF defects, and was referred for evaluation. VA was -0.14 and 0.0 LogMAR at 55 years of age, and 0.0 and 0.18 after four years of follow-up in the right and the left eye respectively. Vessel attenuation, pale discs and inferior RPE granularity were observed on funduscopy and remained relatively stable during follow-up; visible on FAF (**Figure 5F**). ERG at 56 years of age, showed a reduction in rod and cone amplitudes, with no peak-time shift.

**Autosomal Dominant Sector RP*****IMPDH1* (n=3)**

The mean age of presentation was 56.3 years old (range 52.1 - 70.4 years). P11 and P13 were asymptomatic and incidentally noted to have retinal changes. P12 presented with peripheral field constriction and difficulty focusing. The mean presenting VA was 0.06 logMAR (range 0.00 – 0.18 logMAR). Patient P12 had superior visual field constriction to 20 degrees. P11 was the only patient who had an ERG, which demonstrated generalised retinal dysfunction, affecting the rod more than cone systems. None of the patients had foveal involvement or progression on FAF (**Figure 2G and 5G**).

***RP1* (n=3)**

The mean age of presentation was 33.1 years-old (range 26.0 – 41.1 years). The mean presenting VA was 0.06 logMAR (range 0.00 – 0.18 logMAR). On ERG, P14 had generalized dysfunction of the rod system and P16 had generalised retinal dysfunction of both rod and cone systems. Two of the patients showed evidence of mild progression on FAF (**Figure 5H-I**).

***RHO* (n=10)**

Patients with *RHO* variants had a mean age of presentation of 52.2 years-old (range 28.6 – 61.7 years). Four patients presented with nyctalopia, five presented with peripheral visual symptoms, and the final patient was asymptomatic. The mean presenting VA was 0.03 logMAR (range 0.00 - 0.24 logMAR). None of the patients had foveal involvement, and only one had evidence of mild progression on FAF (**Figure 5J**).

## DISCUSSION

Herein, we investigated the genetic and phenotypic variation in the largest cohort of molecularly confirmed patients with sector RP in the literature. We identified nine genes as causative for the disease, of which five were not previously implicated (*PRPS1*, *MYO7A*, *EYS*, *IMPDH1*, and *RP1*). We provided data for disease natural history and information that can help inform patient counselling and prognosis for each individual genotype.

Sector RP has a favourable visual prognosis compared to “typical” RP. It has been reported that 82% of patients retain a VA of 0.3 LogMAR or better (n=17, not molecularly confirmed).<sup>27</sup> In our cohort, 24 patients (24/26, 83.3%) had VA better than 0.3 LogMAR (**Figure 1**). Coussa *et al.* recently reported that those with sector RP due to *RHO* (n=9) retain relatively good central vision (better than 0.18 LogMAR). In agreement with the aforementioned study, 87.5% (7/8) of our patients with *RHO* variants had VA equal or better than 0.18 LogMAR. In our cohort, relative structural and functional stability was observed across all genotypes during follow-up (**Figure 1** and **Figure 5**). We recently reported 105 affected families with *RHO*-associated disease in our genetic database;<sup>28</sup> in the current report we associate 8 of them with sector RP (7.6%). A predisposition for inferior and/or nasal retinal involvement has been reported for sector RP due to *RHO*,<sup>6</sup> and that was also observed in all the cases in the current report. There are on-going human clinical trials of antisense oligonucleotide therapy and hydroxychloroquine (NCT04123626 and NCT04120883 respectively) for patients harboring the *RHO* variant P23H. This variant has also been reported in sector RP.<sup>6, 8</sup> None of our 8 families harboured P23H; with this variant being common in the USA. Overall, our data support that most patients with sector RP, albeit with a degree of variability depending on the genotype, can be advised of a good prognosis, with serial monitoring for progression with wide-field imaging and for secondary complications with OCT (e.g. CME, **Figure 5F**).

*RPGR*-associated sector RP appears to have distinct features from other genotypes and a worse prognosis. Two patients are reported in the literature with *RPGR* variants and sectoral disease (**Table 1**); one patient had impaired central vision with asymmetry between the eyes (0.48 and 1.3 LogMAR),<sup>4</sup> and the other was described as having cone-rod dystrophy (rather than RP=rod-cone dystrophy) and sectoral disease, presenting also with impaired central vision.<sup>21</sup> *RPGR* patients (n=3) tended to have worse VA for their age in the cohort (**Figure 1**). Asymmetry in VA, was noted in P4 over the follow-up (0.4 LogMAR interocular difference), and can be attributed to foveal involvement, where small structural changes can have a more dramatic effect on VA. Both of the aforementioned patients in the literature (reported recently from two independent centers), and our P3 had a small deletion leading to a frameshift at the same location (c.3092). It should also be highlighted that P2 was an *RPGR* carrier and to the best of our knowledge is the first reported carrier with sector RP (**Figure 2A**). In all the reported patients with *RPGR* variants, the changes are primarily nasal and peripapillary (**Figure 2A-C**). Trials of gene augmentation therapy are already underway for *RPGR*-associated RP (NCT03252847, NCT03116113, and NCT03316560).

Usher syndrome is genetically and phenotypically heterogeneous, and with the current report we further extend the phenotypic spectrum of the retinal manifestations of

the causative genes. *USH1C* causes Usher type 1C (USH1C, OMIM 276904), and has previously been associated with sector RP (P5 and P6 in the current study).<sup>2</sup> *MYO7A* and *CDH23* are causes of USH1B (OMIM 276900) and USH1D (OMIM 601027) respectively. P7 and P8 with *MYO7A*, had severe congenital hearing loss, could articulate and wore hearing aids, suggesting some useful hearing, which is not typical in USH1B. In keeping with the milder hearing deficit, retinal disease was also mild and limited to the inferior retina. Both patients have minimal ERG abnormality, in contrast to the usually undetectable responses in *MYO7A*-associated USH1B (88.6%).<sup>29</sup> Three of the four variants identified in P7 and P8, are missense changes and may represent hypomorphic alleles, thereby allowing residual cochlear function and sector RP. P9 with *CDH23* variants was compound heterozygous for a null and a missense variant. Non-syndromic deafness is associated with *CDH23* missense variants that are presumed to be hypomorphic alleles with sufficient residual activity for retinal function, but not for auditory cochlear function. In contrast, null *CDH23*, or a combination of a null allele and a missense in a compound heterozygote, cause USH1D.<sup>30</sup> Our case is the second case reported in the literature where the combination of a null and missense variant leads to deafness and sector RP (*i.e.* mild retinal manifestations).<sup>18</sup>

*RP1* encodes a microtubule-associated protein which is thought to be retina-specific and sequence variants are known to cause AD and AR RP.<sup>31, 32</sup> Notably, AD *RP1* RP has a relatively mild phenotype, with variants clustered in the large terminal exon 4, as was the case in our patients (P14 – P16). Previously reported variants are usually truncating,<sup>33</sup> as was also the case in our patients. Variants in other exons can cause a more severe phenotype including early-onset retinal degeneration, but only when homozygous.<sup>32</sup> Of note, two of our three patients with *RP1* showed some progression on serial FAF; however, none demonstrated foveal involvement. *IMPDH1* encodes inosine-5-prime-monophosphate dehydrogenase which is responsible for guanine nucleotide biosynthesis. It has been reported to cause AD RP and rarely Leber congenital amaurosis.<sup>34</sup> *IPMDH1-RP* has been attributed to protein misfolding as opposed to reduced enzymatic activity.<sup>35</sup> Sector RP due to *RP1* and *IMPDH1* represent a milder phenotype, with no definite genotype-phenotype association evident, suggesting other modifying molecular or environmental factors.

Light exposure has been implicated given the inferior retinal predilection of sector RP. Light deprivation reduces retinal degeneration in *RHO* related RP animal models.<sup>36</sup> Animal models exhibiting rhodopsin glycosylation deficiency are vulnerable to light related retinal degeneration.<sup>37, 38</sup> This may be clinically relevant, as occupationally related high sunlight exposure may lead to a more severe phenotype, potentially (at least in part) explaining the commonly observed intrafamilial phenotypic variability in *RHO*-RP.<sup>39</sup> While the underlying molecular mechanism remains unclear, it is interesting that the inferior predilection was common among the 9 causative genes identified herein. Speculation of a common / down-stream mechanism of light-induced damage is possible. Gradients of gene expression in the retina that are not normally clinically manifest might also predispose the retinal quadrants differently. Given the current evidence, it is reasonable to also advise patients with sector RP to use protection and minimize light exposure.

Our series highlights that the genotypic spectrum is broader. However, as a single tertiary referral center it is difficult to draw conclusions for disease prevalence

within the general population, as well as about the prevalence of each gene in patients with sector RP, since mild cases or cases with dominant inheritance may lack molecular confirmation. Our study was retrospective, and as a result not all the data were available for all the patients. Further evaluation and quantification of the ERG parameters, and use of wide-field imaging longitudinally will be of value to monitor disease progression.

Herein we presented the largest cohort of molecularly confirmed patients with sector RP. The genotypic spectrum of the disease is broader than previously reported, with 5 novel genes causing sector RP identified. The provided longitudinal data will be valuable to better inform patient prognosis and counselling.

Journal Pre-proof

## **Acknowledgments and Disclosures**

### **Funding**

Supported by grants from the National Institute for Health Research Biomedical Research Centre at Moorfields Eye Hospital NHS Foundation Trust and UCL Institute of Ophthalmology, Onassis Foundation, Leventis Foundation, The Wellcome Trust (099173/Z/12/Z), Moorfields Eye Hospital Special Trustees, Moorfields Eye Charity, Retina UK, Fight for Sight UK, and the Foundation Fighting Blindness (USA).

### **Financial Disclosures:**

Michalis Georgiou and Michel Michaelides consult for MeiraGTx. The following authors have no financial disclosures: PSG, AN, MA, NA, KF, ARW.

### **Conflict of Interest:**

No conflict of interest exist for any of the authors.

### **Authorship:**

All authors attest that they meet the current ICMJE criteria for Authorship.

### **Acknowledgements:**

None

**REFERENCES**

1. Verbakel SK, van Huet RAC, Boon CJF, et al. Non-syndromic retinitis pigmentosa. *Prog Retin Eye Res* 2018;66:157-86.
2. Saihan Z, Stabej Ple Q, Robson AG, et al. Mutations in the USH1C gene associated with sector retinitis pigmentosa and hearing loss. *Retina* 2011;31(8):1708-16.
3. Karali M, Testa F, Brunetti-Pierri R, et al. Clinical and Genetic Analysis of a European Cohort with Pericentral Retinitis Pigmentosa. *Int J Mol Sci* 2019;21(1).
4. Coussa RG, Basali D, Maeda A, et al. Sector retinitis pigmentosa: Report of ten cases and a review of the literature. *Mol Vis* 2019;25:869-89.
5. Bietti G. Su alcune forme atipiche o rare di degenerazione retinica (degenerazioni tappetoretiniche e quadri morbosi similari). *Boll Oculist* 1937(16):1159-244.
6. Stone EM, Kimura AE, Nichols BE, et al. Regional distribution of retinal degeneration in patients with the proline to histidine mutation in codon 23 of the rhodopsin gene. *Ophthalmology* 1991;98(12):1806-13.
7. Grover S, Fishman GA, Anderson RJ, et al. Visual acuity impairment in patients with retinitis pigmentosa at age 45 years or older. *Ophthalmology* 1999;106(9):1780-5.
8. Heckenlively JR, Rodriguez JA, Daiger SP. Autosomal dominant sectoral retinitis pigmentosa. Two families with transversion mutation in codon 23 of rhodopsin. *Arch Ophthalmol* 1991;109(1):84-91.
9. Fishman GA, Stone EM, Gilbert LD, Sheffield VC. Ocular findings associated with a rhodopsin gene codon 106 mutation. Glycine-to-arginine change in autosomal dominant retinitis pigmentosa. *Arch Ophthalmol* 1992;110(5):646-53.
10. Moore AT, Fitzke FW, Kemp CM, et al. Abnormal dark adaptation kinetics in autosomal dominant sector retinitis pigmentosa due to rod opsin mutation. *Br J Ophthalmol* 1992;76(8):465-9.
11. Kranich H, Bartkowski S, Denton MJ, et al. Autosomal dominant 'sector' retinitis pigmentosa due to a point mutation predicting an Asn-15-Ser substitution of rhodopsin. *Hum Mol Genet* 1993;2(6):813-4.
12. Rivera-De la Parra D, Cabral-Macias J, Matias-Florentino M, et al. Rhodopsin p.N78I dominant mutation causing sectorial retinitis pigmentosa in a pedigree with intrafamilial clinical heterogeneity. *Gene* 2013;519(1):173-6.
13. Budu, Matsumoto M, Hayasaka S, et al. Rhodopsin gene codon 106 mutation (Gly-to-Arg) in a Japanese family with autosomal dominant retinitis pigmentosa. *Jpn J Ophthalmol* 2000;44(6):610-4.
14. Ramon E, Cordomi A, Aguila M, et al. Differential light-induced responses in sectorial inherited retinal degeneration. *J Biol Chem* 2014;289(52):35918-28.
15. Napier ML, Durga D, Wolsley CJ, et al. Mutational Analysis of the Rhodopsin Gene in Sector Retinitis Pigmentosa. *Ophthalmic Genet* 2015;36(3):239-43.
16. Shah SP, Wong F, Sharp DM, Vincent AL. A novel rhodopsin point mutation, proline-170-histidine, associated with sectoral retinitis pigmentosa. *Ophthalmic Genet* 2014;35(4):241-7.
17. Xiao T, Xu K, Zhang X, et al. Sector Retinitis Pigmentosa caused by mutations of the RHO gene. *Eye (Lond)* 2018.

18. Branson SV, McClintic JI, Stamper TH, et al. Sector Retinitis Pigmentosa Associated With Novel Compound Heterozygous Mutations of CDH23. *Ophthalmic Surg Lasers Imaging Retina* 2016;47(2):183-6.
19. Sato M, Oshika T, Kaji Y, Nose H. A novel homozygous Gly107Arg mutation in the RDH5 gene in a Japanese patient with fundus albipunctatus with sectorial retinitis pigmentosa. *Ophthalmic Res* 2004;36(1):43-50.
20. Nakamachi Y, Nakamura M, Fujii S, et al. Oguchi disease with sectoral retinitis pigmentosa harboring adenine deletion at position 1147 in the arrestin gene. *Am J Ophthalmol* 1998;125(2):249-51.
21. Nguyen XT, Talib M, van Schooneveld MJ, et al. RPGR-Associated Dystrophies: Clinical, Genetic, and Histopathological Features. *Int J Mol Sci* 2020;21(3).
22. Tee JJ, Smith AJ, Hardcastle AJ, Michaelides M. RPGR-associated retinopathy: clinical features, molecular genetics, animal models and therapeutic options. *Br J Ophthalmol* 2016;100(8):1022-7.
23. Sudharsan R, Beltran WA. Progress in Gene Therapy for Rhodopsin Autosomal Dominant Retinitis Pigmentosa. *Adv Exp Med Biol* 2019;1185:113-8.
24. Fiorentino A, Fujinami K, Arno G, et al. Missense variants in the X-linked gene PRPS1 cause retinal degeneration in females. *Hum Mutat* 2018;39(1):80-91.
25. Mastey RR, Gaffney M, Litts KM, et al. Assessing the Interocular Symmetry of Foveal Outer Nuclear Layer Thickness in Achromatopsia. *Transl Vis Sci Technol* 2019;8(5):21.
26. Kalitzeos A, Samra R, Kasilian M, et al. Cellular imaging of the tapetal-like reflex in carriers of RPGR-associated retinopathy. *Retina* 2019;39(3):570-80.
27. Grover S, Fishman GA, Alexander KR, et al. Visual acuity impairment in patients with retinitis pigmentosa. *Ophthalmology* 1996;103(10):1593-600.
28. Pontikos N, Arno G, Jurkute N, et al. Genetic basis of inherited retinal disease in a molecularly characterised cohort of over 3000 families from the United Kingdom. *Ophthalmology* 2020.
29. Khateb S, Mohand-Said S, Nassisi M, et al. Phenotypic characteristics of rod-cone dystrophy associated with MYO7A mutations in a large french cohort. *Retina* 2019.
30. Schultz JM, Bhatti R, Madeo AC, et al. Allelic hierarchy of CDH23 mutations causing non-syndromic deafness DFNB12 or Usher syndrome USH1D in compound heterozygotes. *J Med Genet* 2011;48(11):767-75.
31. Bowne SJ, Daiger SP, Hims MM, et al. Mutations in the RP1 gene causing autosomal dominant retinitis pigmentosa. *Hum Mol Genet* 1999;8(11):2121-8.
32. Al-Rashed M, Abu Safieh L, Alkuraya H, et al. RP1 and retinitis pigmentosa: report of novel mutations and insight into mutational mechanism. *Br J Ophthalmol* 2012;96(7):1018-22.
33. Nanda A, McClements ME, Clouston P, et al. The Location of Exon 4 Mutations in RP1 Raises Challenges for Genetic Counseling and Gene Therapy. *Am J Ophthalmol* 2019;202:23-9.
34. Bowne SJ, Sullivan LS, Mortimer SE, et al. Spectrum and frequency of mutations in IMPDH1 associated with autosomal dominant retinitis pigmentosa and leber congenital amaurosis. *Invest Ophthalmol Vis Sci* 2006;47(1):34-42.

35. Aherne A, Kennan A, Kenna PF, et al. On the molecular pathology of neurodegeneration in IMPDH1-based retinitis pigmentosa. *Hum Mol Genet* 2004;13(6):641-50.
36. Naash ML, Peachey NS, Li ZY, et al. Light-induced acceleration of photoreceptor degeneration in transgenic mice expressing mutant rhodopsin. *Invest Ophthalmol Vis Sci* 1996;37(5):775-82.
37. Tam BM, Moritz OL. The role of rhodopsin glycosylation in protein folding, trafficking, and light-sensitive retinal degeneration. *J Neurosci* 2009;29(48):15145-54.
38. Tam BM, Noorwez SM, Kaushal S, et al. Photoactivation-induced instability of rhodopsin mutants T4K and T17M in rod outer segments underlies retinal degeneration in *X. laevis* transgenic models of retinitis pigmentosa. *J Neurosci* 2014;34(40):13336-48.
39. Iannaccone A, Man D, Waseem N, et al. Retinitis pigmentosa associated with rhodopsin mutations: Correlation between phenotypic variability and molecular effects. *Vision Res* 2006;46(27):4556-67.

**[FIGURE LEGENDS]****Figure 1: Visual Acuity Graphical Representation**

Twenty four patients had available visual acuity (VA) data, with 20 patients being longitudinally assessed, with a mean follow-up of 10.6 years (range: 2.3-36.1 years). The graph represents VA at baseline and follow-up (where available), over age. Each genotype is presented with a different marker.

**Figure 2: Disease Symmetry**

Fundus autofluorescence imaging of the right and left eyes of ten patients (A-J), with sector retinitis pigmentosa. Disease was symmetric in all the presented cases, with the exception P3 (B). The age and the genotype of each individual is noted in the figure.

**Figure 3: Examples of Disease Asymmetry**

**(A)** *PRPS1* is known to cause asymmetric disease in females, multimodal imaging data were only available from the right eye precluding interocular comparison. Left: Color Fundus photograph (CFP), Right: near-infrared imaging of the right eye with the white line marking the location of the transfoveal optical coherence tomography (OCT) scan presented below. **(B)** and **(C)** examples of interocular asymmetry. **(B)** P3 has more advanced disease nasally in the left eye (white arrow heads), which are better visualised with fundus autofluorescence imaging (second line). **(C)** CFPs of P17, with more advanced disease temporal to the fovea in the right eye (white arrow heads).

**Figure 4: Optical Coherence Tomography (OCT) in Sector Retinitis Pigmentosa**

**(A-F)** Transfoveal horizontal OCT scans of six patients with sector RP, of both eyes at baseline and follow-up. Genotype, age at baseline and follow-up time are noted in the figure. **(A, C and E)** Patients had no foveal involvement and stable disease. **(B)** P4 had foveal involvement, with no evidence of progression over follow-up. **(D)** P13 had vitreomacular traction (VMT; P13, Stage 1 in the right eye). **(A)** P2, **(D)** P13 and **(F)** P26, had varying degrees of cystoid macular edema; with **(D)** likely being secondary to traction.

R: right eye, L: left eye, y:years

**Figure 5: Disease Progression**

Fundus autofluorescence imaging of right or left eyes of ten patients **(A-J)**, with sector retinitis pigmentosa, at baseline and follow-up. The genotype of the patient and the age at baseline and follow-up is noted in the figure. The white arrow heads mark the areas of progression in seven patients. Any noted progression was small in area/extent with most likely no/limited clinical impact.  
yo: years old

**Figure 6: Wide-field imaging in Sector Retinitis Pigmentosa (RP)**

On the left, color fundus photographs of the right and left eyes of five patients with sector RP, and on the right, corresponding fundus autofluorescence (FAF) images. Genotype and age of each patients are presented in the figure. For cases **(A-C)** disease

is extending well below the arcades and it is thereby not possible to fully assess with conventional 55 degree FAF (Figure 2).

Journal Pre-proof

Table 1: Demographics and Genetics

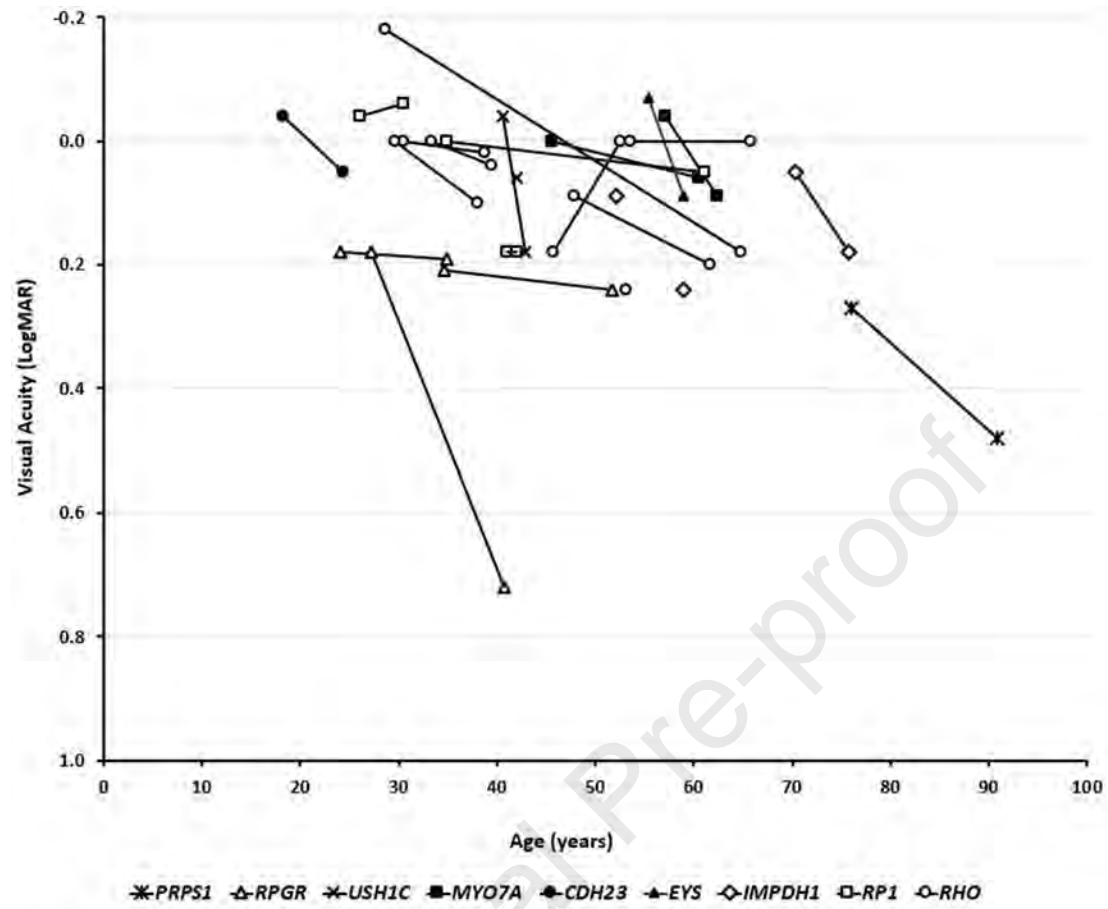
Patient ID	Pedigree	Genetics ID	Genes	Sex	Family History	Variant 1		Variant 2	
						Nucleotide change	Amino acid change/effect	Nucleotide change	Amino acid change/effect
<b>X-linked Sector Retinitis Pigmentosa</b>									
P1	20175	35460	<i>PRPS1</i>	F	Y	c.47C>T	p.Ser16Phe		
P2	1737	21404	<i>RPGR</i>	F	Y	c.1239_1243delAGAGA	p.(Glu414Glyfs*37)		
P3	5345	31560	<i>RPGR</i>	M	N	c.3092delA	p.(Glu1031Glyfs*58)		
P4	4297	26063	<i>RPGR</i>	M	Y	c.485_486delTT	p.Phe162Tyrfs*4		
<b>Autosomal Recessive Sector Retinitis Pigmentosa</b>									
P5	16975	26022	<i>USH1C</i>	M	Y	c.308 G>A	p.Arg103His	c.2227-1G>T	p.?
P6	16975	30346	<i>USH1C</i>	F	Y	c.308 G>A	p.Arg103His	c.2227-1G>T	p.?
P7	20699	31899	<i>MYO7A</i>	F	N	c.3476G>T	p.Gly1159Val	c.3728C>T	p.Pro1243Leu
P8	19131	29686	<i>MYO7A</i>	M	N	c.22dupG	p.Asp8Glyfs*34	c.6551C>T	p.Thr2184Met
P9	21894	33976	<i>CDH23</i>	M	N	c.5237G>A	p.Arg1746Gln	c.9278+2T>G	p.?
P10	22692	34950	<i>EYS</i>	F	Y	c.6794delC	p.Pro2265Glnfs*	c.8278C>T	p.Arg2760Cys
<b>Autosomal Dominant Sector Retinitis Pigmentosa</b>									
P11						c.1074+6_1074+7delGCinsT			
	20700	31900	<i>IMPDH1</i>	M	Y	T	p.?		
P12	18732	28954	<i>IMPDH1</i>	F	Y	c.968A>G	p.Lys323Arg		
P13	24034	37043	<i>IMPDH1</i>	F	N	c.1603A>G	p.Lys535Glu		
P14	3650	2322	<i>RP1</i>	F	y	c.2172_2185del	p.Ile725Argfs*6		
P15	21079	32583	<i>RP1</i>	F	Y	c.2029C>T	p.Arg667*		
P16	18591	28719	<i>RP1</i>	F	Y	c.2206dupA	p.Thr736Asnfs*4		
P17	16765	23876	<i>RHO</i>	F	Y	c.165C>A	p.Asn55Lys		
P18	2482	1535	<i>RHO</i>	M	Y	c.937-1G>T	p.?		
P19	1379	4976	<i>RHO</i>	F	Y	c.410G>T	p.Met39Arg		
P20	1379	22517	<i>RHO</i>	F	Y	c.410G>T	p.Met39Arg		
P21	3509	21686	<i>RHO</i>	F	y	c.568G>A	p.Asp190Asn		
P22	3509	9533	<i>RHO</i>	M	y	c.568G>A	p.Asp190Asn		

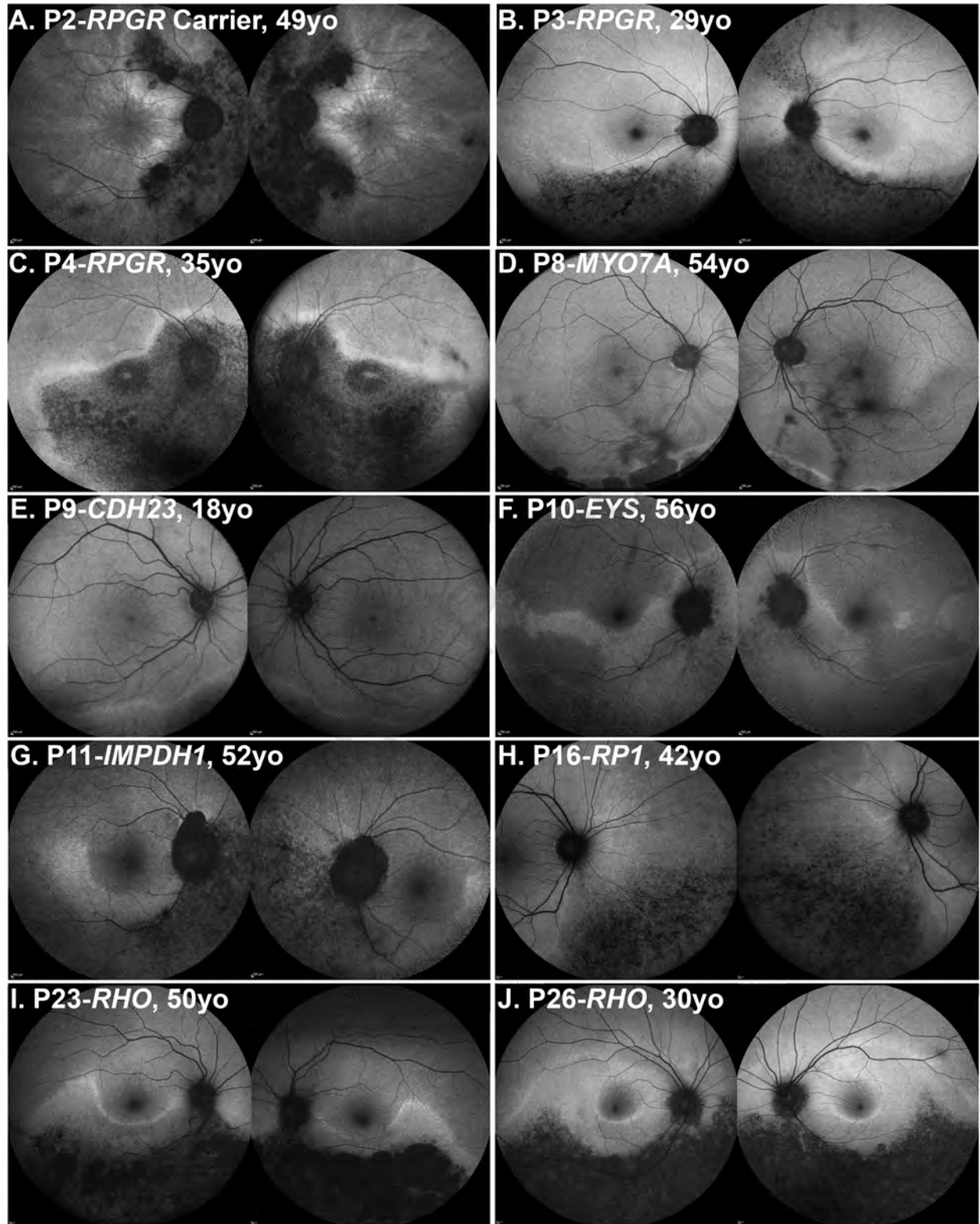
P23	1895	9592	<i>RHO</i>	F	Y	c.316G>A		p.Gly106Arg
P24	3492	10471	<i>RHO</i>	F	N	N	c.467C>G	p.Thr58Arg
P25	2554	9924	<i>RHO</i>	F	Y	N	c.568G>A	p.Asp190Asn
P26	19172	29744	<i>RHO</i>	M	y	N	c.116T>G	p.Met39Arg

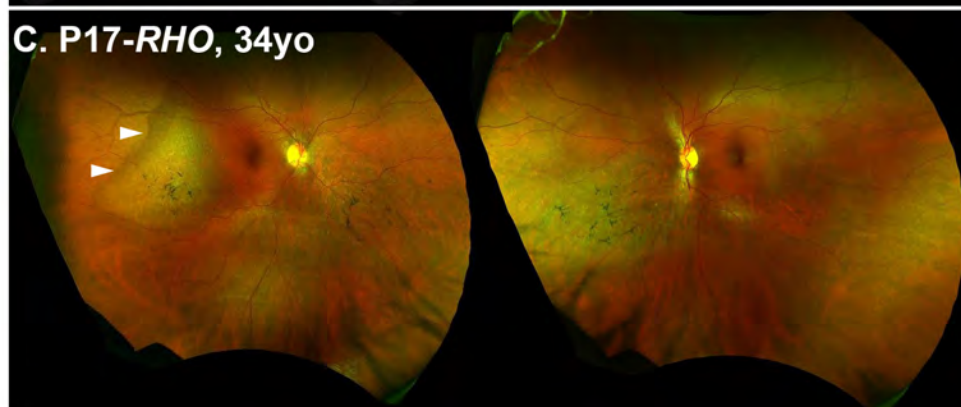
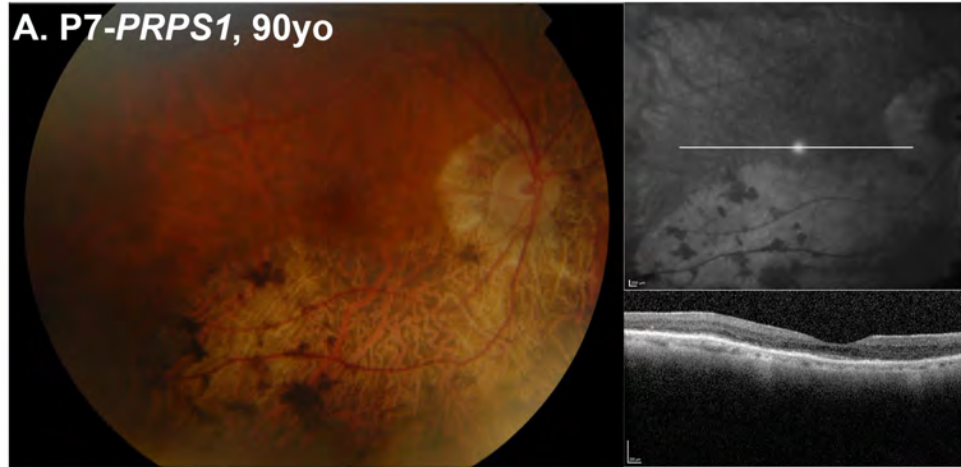
---

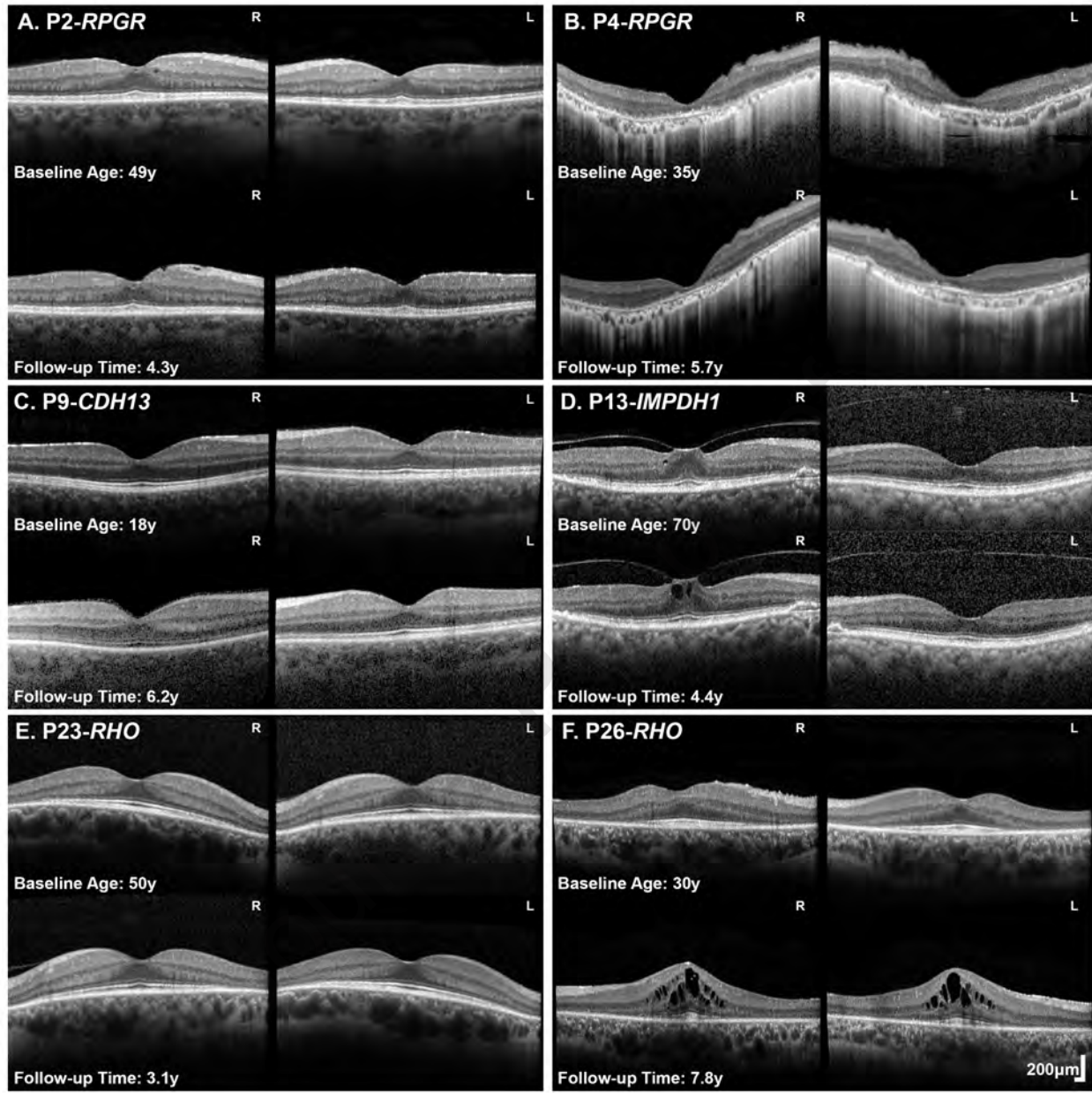
Transcript ID: PRPS1 (NM\_002764.4); RPGR (NM\_001034853.2); USH1C (NM\_153676.4); MYO7A (NM\_000260); CDH23 (NM\_022124.6); EYS (NM\_001142800.1); IMPDH1 (NM\_000883.4); RP1(NM\_006269.2); RHO (NM\_000539.3)

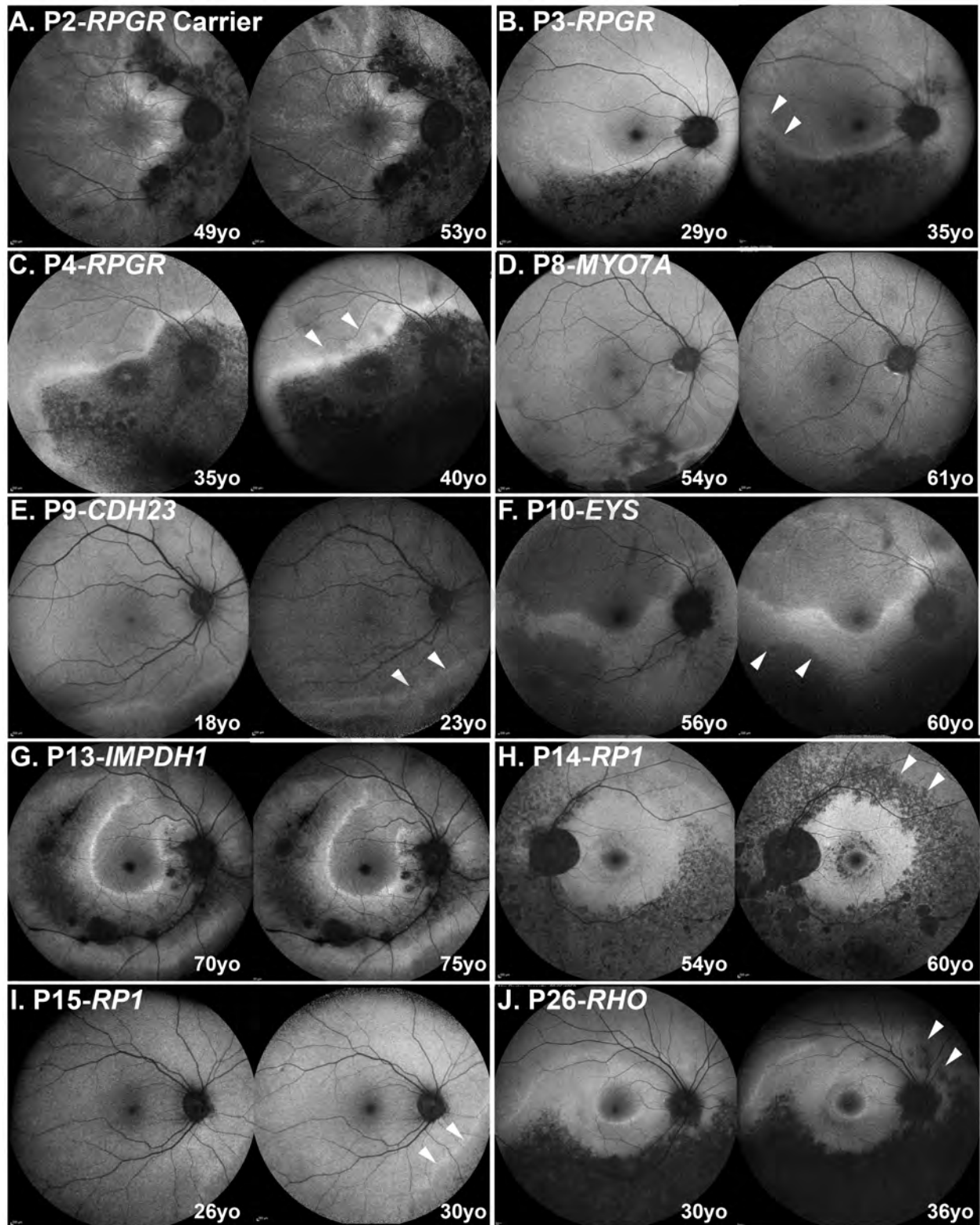
Journal Pre-proof

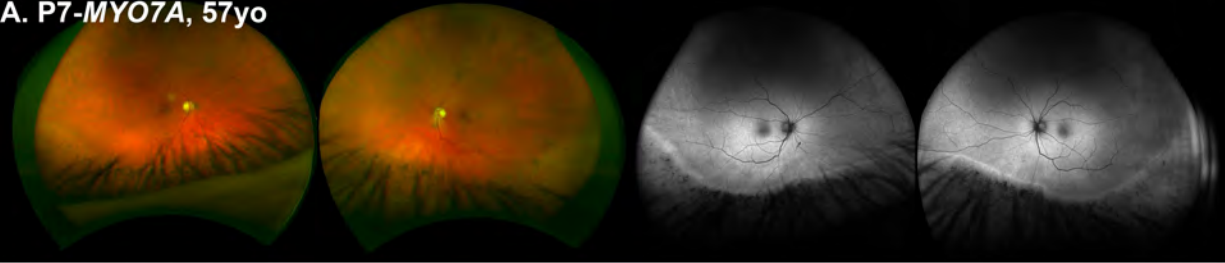
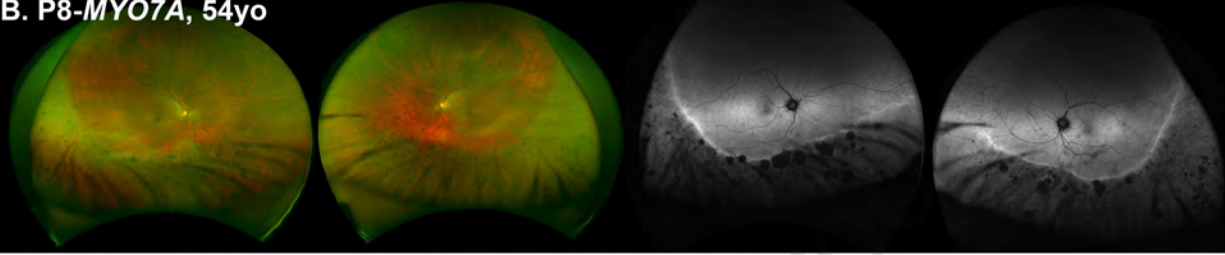
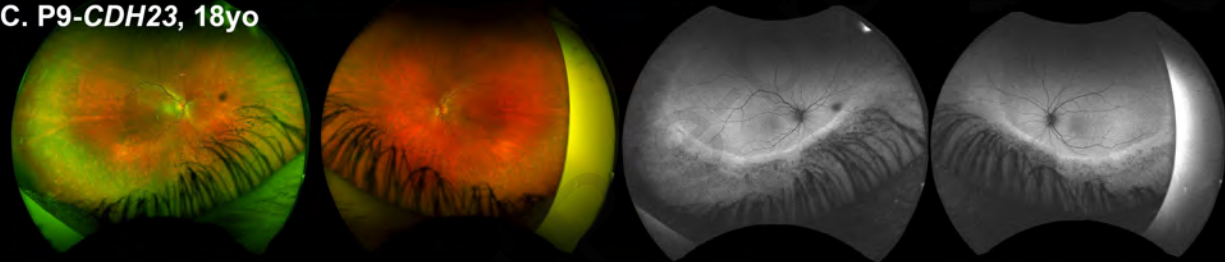
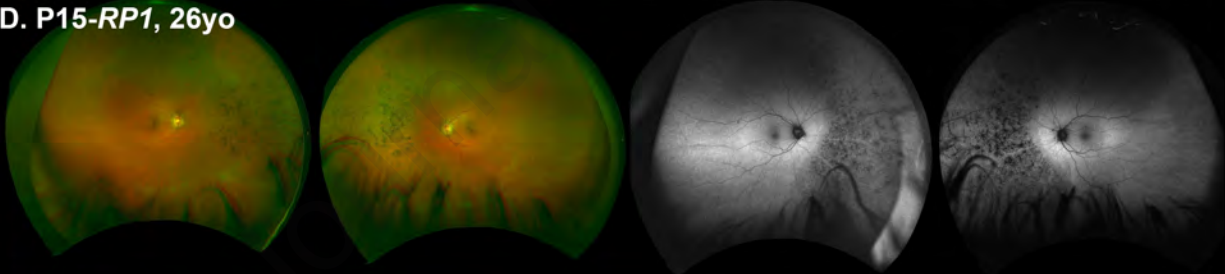
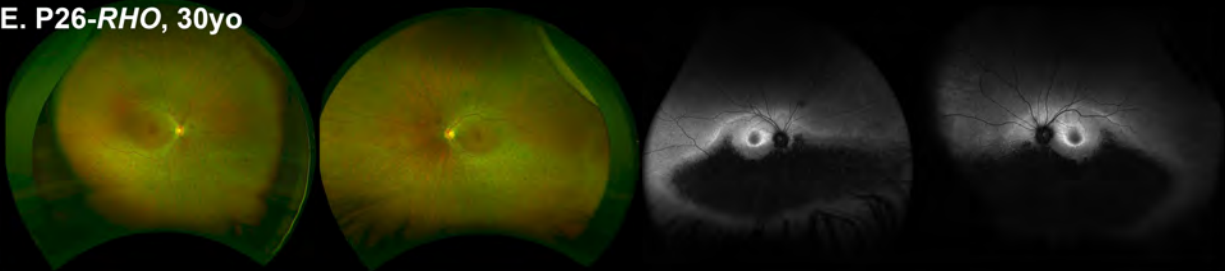










**A. P7-MYO7A, 57yo****B. P8-MYO7A, 54yo****C. P9-CDH23, 18yo****D. P15-RP1, 26yo****E. P26-RHO, 30yo**

## Highlights

- This is the largest series and longitudinal study in sector retinitis pigmentosa.
- The genotypic spectrum of the disease is broader than previously reported.
- The provided longitudinal data provide more accurate patient prognosis and counselling.
- The study inform patients' potential participation in the increasing numbers of trials of novel therapeutics and access to future treatments.